

The Energetics and Electronic Structure of Defective and Irregular Surfaces on MgO

L. N. Kantorovich*, J. M. Holender and M. J. Gillan
Physics Department, Keele University
Keele, Staffordshire ST5 5BG, U.K.

November 6, 2018

Abstract

Ab initio calculations based on the density-functional pseudopotential approach have been used to study the fully relaxed structure, the electron distribution and the electronic density of states of (001) terraces, steps, corners and reverse corners, and of F-centers at these surface features on MgO. The calculations confirm earlier predictions of the relaxed structures of surface irregularities based on simple interaction models. A substantial narrowing of the band-gap is found at the surface, which for terraces and steps is due to surface states at the bottom of the conduction band, but for the corner and reverse corner is also due to surface states at the top of the valence band. The F-center formation energy decreases steadily as the coordination of the oxygen site is reduced. The energy of the F-center level shows a tendency to approach the top of the valence band as the coordination of its site decreases.

1 Introduction

There is a general consensus that surface defects such as steps, kinks, corners and surface anion and cation vacancies play a crucial role in molecular processes at oxide surfaces [1, 2, 3, 4, 5, 6, 7]. Yet in a very general sense the background understanding needed to discuss these processes is seriously lacking. There is very little direct experimental information about the structure and energetics of these surface defects for most oxides (see, for instance, references [2, 4]). It is true that there has been useful theoretical work on the relaxed structure of steps and other surface irregularities (see e.g. references [7, 8, 9]) based on simple (and usually empirical) interaction models, but the validity of the assumptions on which the models are based is not always clear. Important insights have also been gained *via* semi-empirical quantum

*On leave from University of Latvia, 19 Rainis, Riga, LV-1050, Latvia

calculations [3, 10, 11, 12]. In a few cases, fully *ab initio* calculations on oxide surfaces have been reported [13, 14, 15, 16, 17, 18, 19], but these are almost all restricted to flat non-defective surfaces (see, however, Ref. [13, 19]).

The aim of the present paper is to contribute to the background understanding of defective oxide surfaces by reporting a series of *ab initio* total-energy calculations on the relaxed atomic structure and the electronic structure of the flat MgO (001) surface, of steps, corners and reverse corners (see Section 5 for the complete explanation of these terms) on this surface, and of surface F-centers (two electrons trapped in an oxygen vacancy) at the flat surface and at the step, corner and reverse corner. For reference purposes, we also present results on the bulk F-center. Our particular interest is in the processes of oxygen exchange between the gas phase and the crystal lattice, and the present work is intended to provide some of the essential information needed for describing these processes, but we believe our results will also be relevant to other problems, such as the interpretation of the spectroscopic properties of the MgO surface.

Our calculations are based on the density-functional pseudopotential approach [20, 21, 22] which has already proved highly successful in many previous studies of oxide surfaces [15, 23, 24] and point defects in oxides [25, 26]. In order to treat defective and irregular oxide surfaces, one needs to do large numbers of calculations on systems containing up to ca. 60 atoms with full relaxation of the system to mechanical equilibrium. With the *ab initio* techniques used in the present work, this can now be done fairly routinely.

The paper is organized as follows. In the following section, we summarize the techniques we have used for calculating the ground-state total energy of the system and the electronic density of states. We then present our results on the bulk F-center (Section 3). This is followed by a description of our results for the flat (001) surface with and without F-centers (Section 4) and for the step, corner and reverse corner and for F-centers at these features (Section 5). A discussion of our results is given in Section 6.

2 Methods

2.1 Total energy calculation

Density-functional theory and the pseudopotential approximation are well established and widely used methods, which have been extensively reviewed in the literature (see e.g. references [20, 21, 22]). Only valence electrons are represented explicitly in the calculations, the valence-core interaction being described by non-local pseudopotentials which are generated by *ab initio* calculations on isolated atoms. The effects of electron correlation are included using the local density approximation (LDA). A large amount of work on MgO based on this approach has already been reported [14, 15, 18, 26, 27, 28, 29, 30, 31, 32]. The calculations are performed on periodically repeated cells, with every occupied valence orbital represented as a plane-wave expansion. This expansion includes all plane waves whose kinetic energy $E_k = \hbar^2 k^2 / 2m$

(\mathbf{k} the wavevector, m the electronic mass) satisfies $E_k < E_{cut}$, where E_{cut} is a chosen plane-wave cut-off energy. This means that calculations can be taken to convergence with respect to the size of basis set simply by increasing the cut-off.

In the present work, the self-consistent ground state of the system is determined using the Car-Parrinello approach [33], in which the total energy is minimized with respect to the plane wave coefficients of the occupied orbitals, the minimization being performed by the conjugate-gradient technique [22]. The calculations were performed with the code CETEP running on the Cray T3D parallel supercomputer at the Edinburgh Parallel Computer Centre. The computational strategy underlying the CETEP code has been described in the literature [34], but the code has been extensively rewritten to take full advantage of the T3D. The main change concerns the way the conjugate gradient search is done. In previous versions, each band was updated sequentially in the iterative search for the ground state. In the version used here, all occupied bands are updated simultaneously. This method exploits the large memory available on the T3D, and results in a speed-up of about a factor of three for the present type of problem.

Technical details of the calculations are as follows. The pseudopotentials for Mg and O atoms are identical to those used in our recent calculations on the adsorption of NH_3 at the MgO (001) surface [15]. As in that work, the Kleinman-Bylander representation [35] of the pseudopotentials is used, with the s component treated as local for Mg and the d component for O. The only difference with this work lies in using the real-space representation [36] of the pseudopotentials, which speeds up the calculations significantly for systems of the large size treated here. We demonstrated in our earlier work [15] that with a plane-wave cut-off $E_{cut} = 600$ eV the total energy is essentially perfectly converged with respect to the size of the basis set, and the same cut-off has been used here. Electronic exchange and correlation are represented by the commonly used Ceperley-Alder form [37, 38]. Brillouin zone sampling for the ground state calculations is performed using the Monkhorst-Pack scheme [39], as noted in more detail later. It was found in our previous calculations [15] that in equilibrium the nearest-neighbor distance is $d = 2.082$ Å, and we have used the same value in our present calculations. Note that it is close to the experimental value 2.105 Å [40].

2.2 Electronic density of states (DOS)

For all systems studied in this paper we have calculated the electronic density of states (DOS)

$$\mathcal{N}(\epsilon) = \frac{1}{N} \sum_{n\mathbf{k}} \delta(\epsilon - \epsilon_{n\mathbf{k}}), \quad (1)$$

where $\epsilon_{n\mathbf{k}}$ is the eigenvalue of the Kohn-Sham equation for the band n and the wave vector \mathbf{k} in the Brillouin zone (BZ) of the supercell, N is the number of unit cells in the crystal. When making calculations on *bulk* systems, the standard tetrahedron method has been used [41, 42]. First, we note that the BZ can be chosen as a parallelepiped defined by the three primitive reciprocal lattice vectors \mathbf{B}_1 , \mathbf{B}_2 , \mathbf{B}_3 .

Then, we divide the BZ into small parallelepipeds of an equal volume by dividing every lattice vector \mathbf{B}_i ($i = 1, 2, 3$) by integers n_1, n_2, n_3 . Every small parallelepiped is then split into six tetrahedra of an equal volume [43], and all the \mathbf{k} -points at the edges of the tetrahedra form a submesh of \mathbf{k} -points. Using the point-group symmetry operations of the system, a significantly reduced set Π of symmetry inequivalent \mathbf{k} -points is obtained, and an array containing the correspondence between these \mathbf{k} -points and all edges of all the tetrahedra is generated. Then, using the CASTEP code [22], we calculate the eigenvalues $\epsilon_{n\mathbf{k}}$ for every \mathbf{k} -point belonging to the set Π . Using the array which sets up the correspondence between the set Π and all edges of tetrahedra, the total DOS is finally calculated.

Several points are worth mentioning. First, we emphasize that for systems of the size treated here the calculations of the eigenvalues $\epsilon_{n\mathbf{k}}$ are extremely demanding and we had to restrict our \mathbf{k} -point sampling by choosing equal divisions $n_1 = n_2 = n_3 = 5$ corresponding to 750 tetrahedra in the whole BZ. For high-symmetry systems without an F-center (except for the perfect corner - reverse corner system which has no symmetry at all) we have used also a larger number of divisions to study the convergence of the total DOS. We found this division to be reasonable and reliable as far as the boundaries and the general structure of bands are concerned. However, we cannot rely on the fine structure of the total DOS since the energy resolution appears to be not completely satisfactory. Second, when making DOS calculations for the surface systems in slab geometry, it is unnecessary to consider the \mathbf{k} -point sampling along the direction of the normal to the surface [15], so that the BZ is reduced to the two-dimensional *surface* BZ. In this case, the method of tetrahedron is simplified to the triangle method. Third, since the \mathbf{k} -point sampling was not very extensive in all our calculations, we found that often there is an accidental equivalence of some edges of one and the same tetrahedron which results in an accidental degeneracy of the eigenvalues, $\epsilon_{n\mathbf{k}}$. This forced us to modify slightly the standard method of tetrahedra to cope with this problem. Namely, we have formally removed this degeneracy by adding different $\delta_\alpha > 0$ to the eigenvalues belonging to the equivalent edges. Then, using equations of the standard method, the corresponding modified formulae have been worked out by making the limit $\delta_\alpha \rightarrow +0$.

3 The bulk F-center

We have used the techniques described in the previous section to perform calculations on the bulk F-center using repeating cells containing 8, 16, 32, 54 and 64 lattice sites. These are all the repeating cells containing between 8 and 64 sites, which preserve the O_h symmetry of the F-center, and they give periodic arrays of F-centers having s.c., f.c.c., b.c.c., f.c.c. and s.c. translational symmetry, respectively. The next available size of the cell would contain 128 sites. For each repeating cell we have first calculated the total energy of the perfect crystal. We have then removed an oxygen atom and repeated the calculation. In addition to treating the unrelaxed F-center, we have also

studied its equilibrium by relaxing all ions in the system. All calculations have been performed using the lowest-order Monkhorst-Pack set of \mathbf{k} -points, consisting of the eight points $(\pm\frac{1}{4}, \pm\frac{1}{4}, \pm\frac{1}{4})$ (in units of the primitive reciprocal lattice vectors). As usual, it is unnecessary to include \mathbf{k} -points related by inversion symmetry, so that the calculations are actually performed with the four points $(\frac{1}{4}, \pm\frac{1}{4}, \pm\frac{1}{4})$.

We first report our results for the oxygen removal energy. This is defined to be the energy (per cell) of the system containing the F-center, plus the energy of an isolated oxygen atom minus the energy of the perfect crystal calculated with exactly the same cell. In view of the large energies involved, it is important that the same cell be used for the F-center and perfect crystal to ensure cancellation of errors. The energy of the isolated oxygen atom was obtained by calculations on a number of periodic systems containing one oxygen atom per cell. The final size of the repeating cell in these calculations has been taken large enough to ensure that the interaction between oxygen atoms introduces an error of less than 0.01 eV. Since an oxygen atom in the ground state has a multiplet structure 3P_2 [44], and the state calculated by the LDA method belongs to the excited state 1D of the atom, a correction has to be made for the energy of the oxygen atom. As an estimate for this correction, we have used the experimental energy difference for these states [44] which is 1.967 eV. Note that the local spin density (LSD) calculations give a somewhat similar correction (the difference between energies calculated using LSD and LD methods) which is 1.496 eV [27, 28] and 1.4 eV [45].

To estimate the overall error in our oxygen removal energies, we have also calculated the cohesive energy (per formula unit with respect to free neutral atoms) of the MgO crystal. Using the total energy of the largest repeating cell for the bulk containing 64 sites and the calculated total energies of the O and Mg atoms, we have calculated the cohesive energy to be 11.14 eV. Note that we have also used the 0.14 eV correction [27] for the zero-point vibrational energy of MgO. Our value turns out to overestimate the experimental cohesive energy (10.3 eV [46]). The existence of this discrepancy with experiment of 0.8 eV suggests that there may be a similar systematic error in calculated oxygen removal energies.

Our calculated oxygen removal energies for both the unrelaxed and relaxed F-center are reported in Table 1. Two main conclusions are clear from these results. First, the removal energies are completely converged with respect to the size of the cell already for the 16-site system. In fact, even the 8-site result differs from the others by only 0.1 eV. Second, the effect of relaxation is completely negligible. The almost complete absence of relaxation effects for the neutral F-center in MgO has also been demonstrated by earlier calculations [28, 30, 47, 48]. The comparison of our calculated oxygen removal energy with experiment and with other calculations will be discussed later.

Although the relaxations are extremely small, they do show systematic behaviour for all the sizes of cell we have studied. The Mg ions adjacent to the F-center relax outwards by an amount which is 0.01 Å for the 54-site and 64-site cells and is somewhat smaller for the smaller cells. The oxygens nearest to the F-center relax outwards by about 0.005 Å for the two largest cells. The relaxations surrounding the F-center in

MgO have been studied previously by *ab initio* calculations [28, 30, 47, 48, 49]. All these calculations agree that the displacements are extremely small and of the same general magnitude that we have found, but there are some disagreements about the directions of the displacements. These disagreements cannot be considered very significant, given the very small effects involved.

We have calculated the electronic DOS for the perfect crystal and for the system containing an F-center, using the tetrahedron technique described in the previous Section. It is straightforward to use enough \mathbf{k} -points to obtain good energy resolution for the perfect crystal, but the calculations on large cells are much more demanding, and the energy resolution for the F-center systems is less good. We show in Fig. 1 our results for the DOS of the perfect crystal and for the 16-site and 54-site F-center systems.

As is well known from many previous calculations, the valence DOS of the perfect crystal consists of a rather narrow band of O(2s) states, and a broader two-peak band of O(2p) states. We have found in our calculations that the widths of these bands are 2.1 eV and 4.9 eV, respectively, and we estimate the separation between two peaks in the band of O(2p) states to be ca. 3.2 eV. Our calculated separation between bands of O(2s) and O(2p) states is ca. 11.3 eV. The widths, positions and shapes of the valence bands in the DOS are in close agreement with previous theoretical results [14, 27, 32, 45, 50]. Agreement with experiment [51, 52, 53, 54] (2.0 - 2.5 eV and 5.0 - 7.0 eV for the widths of the two bands and 13 - 14.5 eV for the *s-p*-bands separation) is somewhat worse but this is usual with LDA calculations. In addition, the bulk band gap between the top of the upper valence band and the bottom of the conduction band is underestimated. Our calculated value is 4.8 eV, which should be compared with the experimental value of 7.8 [55] (note that a bigger value 8.7 eV is reported in [4]). This degree of underestimation of band gaps is very typical for LDA calculations.

The states associated with the F-center are clearly visible in the lower half of the band gap in Fig. 1. An isolated F-center would have a single sharply defined level. In the periodic systems treated here, this level is broadened into a band. As expected, this band is broader for the smaller system. The width of this band is 1.6 eV and 0.6 eV for the 16-site and 54-site systems. The large width for the small system suggests that the F-center wavefunction is rather extended, and we shall analyze this question below. The average energy (i.e. the first moment) of the F-center band is ca. 2.5 eV above the valence band maximum (VBM) for the 16-site system and 2.7 eV above the VBM for the 54-site system. This can be compared with the position deduced from optical absorption measurements. The observed F-center absorption energy is ca. 5.0 eV [56, 57, 58, 59] and it is generally agreed [57, 59, 60] that this represents a transition from the ground state to a state lying just below the conduction band. Taking the band gap to be 7.8 eV [55], we deduce that the F-center level should be roughly 2.8 eV above the VBM. Our calculated position of the F-center level is also in close agreement with values obtained in other *ab initio* calculations (2.34 eV [28], 2.55 eV [29]).

A contour plot of the valence electron density in the 54-site F-center system is shown in Fig. 2. As expected from earlier work [28], the density has a maximum at the center

of the vacancy, but the electron distribution in the vacancy region is rather broad. To understand this in more detail, it is useful to compare the electron distributions in the F-center system and the perfect crystal. We have done this by calculating for each system the total valence charge inside spheres of different radii R centered at the vacancy. We denote this total charge by $n_F(R)$ for the F-center system and $n_P(R)$ for the perfect crystal. We are interested in finding out how rapidly the disturbance due to the F-center dies away with increasing radius. We therefore subtract $n_P(R)$ from $n_F(R)$. To allow for the fact that there are six more electrons in the perfect crystal, it is convenient to study the quantity

$$\Delta n(R) = n_F(R) - n_P(R) + 6. \quad (2)$$

With this definition, $\Delta n(R)$ should tend to zero for large R . Our results for $\Delta n(R)$ are shown in Fig. 3. These results show that the electron distribution outside a radius of approximately 2.0 Å is essentially the same in the F-center system as in the perfect crystal. Bearing in mind that the distance to the nearest Mg ion is 2.08 Å, this rather good localization of the charge associated with the F-center explains the almost complete absence of relaxation effects.

We have also investigated the electron density associated with the F-center band itself. A contour plot of this density is shown in Fig. 4. It is clear from this plot that the density of the F-center band is not completely localized in the vacancy, but has considerable weight on the nearest and even next-nearest oxygen ions. We have analyzed this quantitatively and found that there is roughly one electron in the vacancy, 0.3 electron on nearest oxygens and the remaining 0.7 electron is distributed in weak features in a more distant regions. This indicates that the electron density on oxygen neighbors is associated with states both at the valence band energies and also at the energy of the F-center level. Conversely, the electron density in the vacancy is associated with states both at the energy of the F-center level and also at the valence-band energies. These results are in accord with the calculations of Wang and Holzwarth [28].

4 F-center at the flat (001) surface

4.1 The perfect surface

Before describing our calculations on the surface F-center, we present briefly our results for the perfect surface. In all our surface calculations, we use slab geometry, so that the system we study is a periodically repeated stack of slabs separated by vacuum layers. For the calculation on the perfect surface, we use a vacuum width of 4.164 Å, which our previous work [15] on the MgO (001) surface showed to be enough to make the interaction between slabs negligible. In the present calculations, we have studied slabs containing 2, 4 and 6 layers with 16, 32 and 48 ions respectively in the surface unit cell, and we found that the properties of interest are essentially the same in all three cases.

We have performed \mathbf{k} -point sampling using the lowest-order Monkhorst-Pack scheme. Since sampling along the surface normal is unnecessary [15], this means that we use the two \mathbf{k} -points $(\frac{1}{4}, \pm\frac{1}{4}, 0)$ where the third component is along the surface normal.

There have been a number of experimental studies [61, 62, 63] and previous calculations [7, 15, 16, 64, 65] on the properties of the (001) surface, which indicate that relaxation effects are extremely small. This is fully confirmed in the present calculations. In accord with all previous work, we find that surface oxygens relax outwards and surface magnesiums relax inwards. For the six-layer slab, the values of these displacements are $\epsilon_O = 0.022 \text{ \AA}$ and $\epsilon_{\text{Mg}} = -0.018 \text{ \AA}$. These values are in qualitative agreement with those obtained in our recent pseudopotential LDA calculations [15] using a three-layer slab, which gave $\epsilon_O = 0.032 \text{ \AA}$ and $\epsilon_{\text{Mg}} = -0.003 \text{ \AA}$.

The total electronic DOS for the unrelaxed six-layer slab is shown on the top panel of Fig. 5. The most striking feature is the marked reduction of the band gap. This has a value of 3.2 eV, which is 1.6 eV smaller than our calculated value for the perfect crystal. The figure indicates that the gap states are pulled down from the conduction band, rather than splitting from the top of the valence band.

Our results concerning the reduction of the band gap as one goes from the bulk to the surface are in good agreement with the measurements by energy-dependent electron-energy-loss spectroscopy (EELS) [2, 66] where a 2 eV reduction of the band gap has been observed. A reduction of the band gap has been also obtained in a number of previous calculations [3, 14, 65, 67] though the calculated values differ. For example, surface states below the bottom of the conduction states were found in recent *ab initio* calculations [14], which gave the reduction of the band gap by ca. 0.6 eV. We shall return to the discussion about the surface states in Section 6.

In some oxides, it has been found [68] that the change of the Madelung potential at the surface causes the O(2s) states of surface oxygens to split off from the top of the O(2s) band. We do not observe this in the present case. This is because the Madelung potential is almost unchanged at surface oxygen sites (the Madelung constant at a (001) surface site in the rock-salt structure is 1.682 [69], while the value at a bulk site is 1.748) and that is consistent with the absence of oxygen-based surface states.

We have investigated the nature of the surface states by calculating the fictitious charge density associated with several of the lowest unoccupied bands. In practice, we have calculated the quantity $\rho_i(\mathbf{r})$ defined by

$$\rho_i(\mathbf{r}) = \sum_{\mathbf{k}} w_{\mathbf{k}} \left| \psi_{i\mathbf{k}}(\mathbf{r}) \right|^2, \quad (3)$$

where $\psi_{i\mathbf{k}}(\mathbf{r})$ is the eigenfunction of band i at wavevector \mathbf{k} from the irreducible wedge of the BZ, and $w_{\mathbf{k}}$ is the weighting factor for this wavevector. The quantity $\rho_i(\mathbf{r})$ represents the electron density that would be associated with orbital i if the orbital were occupied. Fig. 6 shows $\rho_i(\mathbf{r})$ for the lowest unoccupied band, i.e. the band immediately above the top of the gap. The localization of $\rho_i(\mathbf{r})$ in the surface region confirms that this band consists of surface states. In contrast to the results of another

ab initio LDA calculation [14] where surface states were found to be predominantly of Mg *s* character, our surface states are concentrated mainly on surface oxygens and above surface magnesiums. The anisotropic nature of $\rho_i(\mathbf{r})$ around the Mg ions can be understood in tight-binding terms as arising from the mixing of Mg(3s) and Mg(3p) states because of the electric field at the surface. This mixing will also cause a lowering of one of the 3s/3p hybrid states, and this is one way of understanding the appearance of gap states below the conduction band minimum (cf. discussion in references [2, 3]).

We have also examined the valence electron density in the surface region, but we do not show it here, since the surface distribution will become clear in the next Section.

4.2 The surface F-center

We have investigated the properties of surface F-centers using calculations on 2-layer, 4-layer and 6-layer slabs. The same surface unit cell was used in all cases. The translation vectors joining nearest neighbor F-centers are in the (110) direction, and their length is $2\sqrt{2}d$, where d is the cation-anion separation in the perfect crystal. With this surface unit cell, the repeating unit contains 16, 32 and 48 sites in the three slabs. For the 4-layer slab, we have studied F-centers both in the surface layer and in the layer immediately below the surface, and for the 6-layer slab, we have also studied the F-center in the third layer. Each repeating unit contains only a single F-center, so that the slab contains an F-center only at one of the surfaces. The vacuum width and the \mathbf{k} -point sampling are the same as for the calculations on the perfect surface. In all cases we have investigated both the unrelaxed and the fully relaxed systems.

We report in Table 2 two oxygen removal energies for each case. The first removal energy refers to the energy required to extract an oxygen atom from the slab with all atoms held fixed at their perfect lattice positions. The second removal energy refers to the same process except that both the initial and the final systems are fully relaxed. It is the second of these energies that is relevant to the real physical process. Four important conclusions emerge from these results. The first is that relaxation effects are extremely small. The largest difference between the two removal energies is only 0.06 eV, which is insignificant for practical purposes. The second conclusion is that the removal energies are insensitive to the slab thickness. Even for the 2-layer slab the removal energy for the top layer differs by only 0.2 eV from the value for the 6-layer slab. The differences between the 4-layer and 6-layer slabs are even smaller. This indicates that the results are well converged with respect to the thickness of the slab. The third conclusion is that the removal energies for the second and third layers are extremely close to the bulk value of 10.55 eV reported in Table 1. However, the first-layer removal energy of 9.77 eV is substantially lower than the bulk value. This effect is expected because of the 5-fold coordination of the surface oxygen atoms.

As in the case of the bulk F-center, the ionic relaxations are very small. For the third-layer F-center, the relaxations are essentially the same as for the bulk F-center. For the surface F-center, the neighboring Mg ions relax away from the F-center in the plane of the surface by 0.02 Å, which is about twice the relaxation found in the

bulk. In addition, they have a component of displacement along the outward surface normal which is 0.04 Å with respect to their relaxed surface positions. This implies a net outward relaxation of 0.02 Å of these neighboring Mg ions with respect to their positions on the perfect surface. The Mg ion directly below the first-layer F-center relaxes away from the F-center by 0.05 Å. The relaxation of neighboring oxygens is negligible.

The electronic DOS for the systems containing first-layer and third-layer F-centers are shown on the bottom and middle panels in Fig. 5. The DOS for the second-layer F-center is almost the same as for the third-layer case. The electronic level of the unrelaxed first-layer F-center is 2.0 eV above the top of the valence band, which becomes 2.3 eV on allowing the system to relax, so that relaxation effects are significant. This F-center energy is slightly below that of the bulk F-center, which is 2.7 eV above the valence band maximum (see Section 3). So far as we are aware, there is no direct experimental evidence on this question. However, it may be relevant that a downward shift of about 0.2 eV in the luminescence of surface F-centers (with respect to that of bulk F-centers) was observed for MgO in experiments on absorboluminescence [70]. A slight downward shift of about 0.04 eV in the surface F-center absorption band in KCl crystal which is similar to MgO crystal studied here, was also reported in [71]. The shift of the F-center level in the direction of lower energies found in our calculations can be explained by a competition of a number of factors which work in opposite directions. Indeed, it was already mentioned above that the total Coulomb (Hartree) potential becomes weaker as one moves from the bulk to the surface. At the same time, the F-center wave function is more diffuse in this case as can be judged from our F-center electronic density distribution which is discussed below. Both these factors work in lifting up the F-center level. On the other hand, the positive kinetic energy of a more diffuse F-center state becomes smaller which results finally in a small downward shift of the F-center level. For the second layer F-center the unrelaxed and relaxed values for the F-center level above the VBM are 2.5 and 2.56 eV, whereas for the third-layer F-center the value is 2.6 eV, which is very close to the bulk value. It is worth commenting briefly that the band gap for the first-layer F-center system is slightly greater than for the perfect surface (3.5 eV rather than 3.2 eV). Such an effect cannot occur for an isolated F-center, and must be due to the finite concentration of F-centers because of the periodic boundary conditions.

The valence electron density of the system containing the first-layer F-center is shown in Fig. 7. The electronic density shows a maximum near the center of the vacancy, and it is interesting to note that this maximum value (0.13 electrons Å⁻³) is only slightly below the corresponding maximum of the bulk F-center (0.15 electrons Å⁻³). The electronic density decays rapidly along the outward surface normal. The conclusion is that the F-center is highly localized in this 5-fold coordinated environment. We have also examined the electron density of the surface F-center level itself, and we found that it is extremely similar to that of the bulk F-center. The valence electron distributions for the systems containing second and third layer F-centers show no significant differences from the distributions for the bulk F-center. Our results show

that already the third-layer F-center is very similar to the bulk F-center.

5 F-center at surface irregularities

5.1 The perfect step, corner and reverse corner

We have studied three kinds of surface irregularities: the step, the corner and the reverse corner, as shown in Fig. 8. As before, the calculations are done using slab geometry, but the repeating unit is now somewhat more complicated. For the step calculations, we use a repeating cell containing 52 sites with each surface of the slab consisting of terraces of width $3d$, separated by steps of height d . The slab contains four layers of ions and the vacuum width is $3d$. We expect this thickness of the slab to be adequate because the calculations described in the previous Section show that the oxygen removal energy from the flat surface is essentially the same for the 4-layer and 6-layer slabs. In order to achieve this geometry for the step system, the translation vectors \mathbf{A}_i of the supercell are

$$\mathbf{A}_1 = d(3, 2, 1), \mathbf{A}_2 = d(0, 4, 0), \mathbf{A}_3 = d(0, 0, 7). \quad (4)$$

The orientation of the coordinate system corresponding to this choice of the lattice vectors is clear from Fig. 8. (It will be noted that for the perfect step, the vector \mathbf{A}_1 could be equally well be taken to be $d(3, 0, 1)$; the reason for our choice of \mathbf{A}_1 will be explained below.) The corner and reverse corner systems are studied using a repeating cell of 44 sites. Each surface of the slab consists again of terraces and steps, but now the steps zig-zag back and forth along the (100) and (010) directions. Corners and reverse corners alternate, with the distance between each corner and the neighboring reverse corner being $2d$. The slab thickness and the vacuum width are the same as before. The translation vectors of the supercell are

$$\mathbf{A}_1 = d(2, -2, 0), \mathbf{A}_2 = d(2, 3, 1), \mathbf{A}_3 = d(0, 0, 7). \quad (5)$$

The lowest order Monkhorst-Pack set of two \mathbf{k} -points is used.

The relaxation energies of both the step and the corner systems are substantial. For the step system, the total relaxation energy per repeating cell is 1.51 eV, which corresponds to 0.38 eV per ion pair along the length of the step. The total relaxation energy for the corner system is 3.01 eV per cell, or 0.75 eV per ion pair along the length of the zig-zag step.

The ionic displacements away from their perfect-lattice positions for the four inequivalent atoms at the step itself are reported in Table 3. Our results show that the displacements are quite substantial and their general direction is such as to smooth out the discontinuity at the step. The ionic displacements associated with the corner and the reverse corner system are reported in Table 4. Once again, we see substantial displacements having the same general tendency as for the perfect step. It is worth noting that the displacements of the Mg ion number 4 at the bottom of the reverse

corner and of its oxygen neighbors 5 are very small. The step on MgO (001) surface has previously been studied both by empirical modeling [7, 8, 9] and by semi-empirical quantum calculations [11, 12], but we cannot provide a detailed comparison since the displacements have not been reported in these earlier studies. However, the magnitudes and directions of the displacements that can be inferred from the pictorial data given in [7, 8, 9, 11, 12] seem to be in general agreement with those we have found.

The electronic DOS for the relaxed step is almost identical to that of the flat (001) surface, and we do not show it here. Just as for the flat surface, there is a band of surface states pulled down from the bottom of the conduction band. The band gap for the step system is 3.3 eV, which is slightly larger than that for the flat surface (3.2 eV, see Section 4.1), but we do not regard this as significant. Thus, our results on the band gap for the step system do not support experimental suggestion [4] of a substantial 0.85 eV lowering of the excitonic surface states associated with four-fold coordinated oxygens on the surface with respect to those for the flat (001) surface. The only other noticeable effect is a downward shift of the O(2p) valence band with respect to the O(2s) band by about 0.2 eV.

The DOS of the corner - reverse corner system shown in Fig. 9 is much more interesting. First, there is a narrow band of states completely split off from the top of the O(2s) states by ca. 1.0 eV. Second, there is a significant peak at the top of the O(2p) valence band, though this is not split off. Third, there is a band of states split off from the bottom of the conduction band. The gap between the top of the valence band and the lowest of the unoccupied states split off from the bottom of the conduction band is 2.4 eV, which is considerably less than that for the flat surface and the step. The UV diffuse reflectance spectroscopy [4] has also demonstrated almost 2.0 eV lowering of the surface excitonic states attributed to the three-fold coordinated surface oxygen atoms (i.e. at the corners) with respect to the band gap for the flat (001) surface. Previous cluster LMTO calculations [3] which found a substantial reduction of the gap at the corners compared with the flat surface of a cluster are also consistent with our calculations. We think that the appearance of the surface states above the bands of O(2s) and O(2p) states can be simply explained by a drastic decrease of the Hartree potential at the corner site (as follows from [69] (see also [1], p. 117), the Madelung constant at the corner site is only 0.87378, i.e. half the value for the five-coordinated surface site where it is 1.68155). The fact that the surface states are not split off completely from the top of the upper valence band is the result of a more delocalized character of these states in comparison with the O(2s) surface states.

As in the case of the flat surface, we have investigated the nature of the surface states by calculating the electron density associated with them, see Eq.(3). For the step system, we find that the surface states at the bottom of the conduction band are extremely similar to those at the flat surface. For the corner - reverse corner system, the surface states split off from the O(2s) band have *s* character and are strongly localized on the corner oxygens with a substantial contribution from the three nearest oxygens on the terrace underneath. The surface states at the top of the valence band have *p* character and are also localized mainly on the corner oxygens; the axis of the

p-like density distribution passes through the corner site and lies almost in the (111) direction. The states at the bottom of the conduction band are shown in Fig. 10, which indicates that they are strongly associated with Mg ions neighboring the reverse corner, though there is also considerable weight on surface oxygen ions.

The total spatial densities of valence electrons in the perfect step and corner systems do not show very remarkable features. However, in order to provide a point of reference for the F-center densities shown later, we display in Fig. 11 the density associated with the corner system on a plane parallel to the terraces passing through the zig-zag step. It is noteworthy that the large displacement of the corner oxygens leads to a significant build-up of charge between these ions and their oxygen neighbors.

5.2 F-center at the step, corner and reverse corner

We have calculated the energy for removing oxygen from the step, the corner and the reverse corner. In the case of the step, we have positioned the F-centers so as to maximize the separation between them, as shown in Fig. 8a. This is the reason for taking the translation vectors \mathbf{A}_i for the step as shown in Section 5.1 (see Eq.(4)). In Fig. 8b, we show the location of the F-centers at the corner and the reverse corner.

The unrelaxed and relaxed oxygen removal energies are given in Table 5. We note the following points. At the reverse corner, the oxygen removal energy is only slightly less (by 0.4 eV) than its value for the first-layer F-center on the flat surface. In both these cases, the F-centers are 5-fold coordinated. A further reduction of 0.4 eV occurs when the F-center is formed at the 4-fold coordinated step site, and the removal energy decreases by 0.9 eV more when we go to the 3-fold coordinated corner site. Overall, the removal energy is 2.5 eV lower at the corner site than in the bulk. The difference between unrelaxed and relaxed removal energies is very small except for the corner site, where it is a little over 1 eV.

The ionic displacements around the F-center for the step system are reported in Table 3, whereas those for systems with a F-center at the corner and reverse corner sites are given in Table 4. Although the general trend is the same as in all systems discussed so far, namely it is an additional outward movement of nearest Mg ions from the F-center site, the additional displacements are found to be substantial only for the F-center at the step and at the corner.

The electron DOS for the system containing the F-center at the step is shown in Fig. 12. This is essentially identical to the DOS for the perfect step system, except for the presence of the narrow F-center band in the gap. The mean energy of this band lies 2.4 eV above the top of the valence band, which is almost identical to its position for the F-center on the flat surface. The DOS for the F-center at the corner and the reverse corner are shown in Fig. 9. The simplest case to understand is that of the F-center at the reverse corner, for which the DOS is very similar to that of the perfect corner - reverse corner system except for the presence of the F-center band in the gap, whose mean position lies only 0.8 eV above the top of the band of O(2p) surface states. The DOS of the corner F-center is more complicated, because in addition to

the appearance of the F-center band, there also are substantial changes to the surface states. The mean position of the F-center band is 1.7 eV above the top of the band of O(2p) surface states, which is considerably higher than that for the reverse corner case. This can mainly be explained by the reduction of the Hartree potential at the corner site and by the strong delocalization of the F-center wave function associated with the F-center band.

We have also looked at the spatial distribution of some interesting features in the DOS. We found that because of the absence of oxygen atoms at the corner sites on the upper side of the slab, the states associated with the band split off from the top of the O(2s) band have changed their character of localization. Namely, they appear to be more delocalized over a larger number of oxygens which are behind the “empty” corners on the same terrace. The localization of these states in the two lowest layers is not changed. Surprisingly, the energy position of this band is also not changed with respect to that for the perfect corner - reverse corner system. In addition to that, we have found similar changes in the nature of states associated with the surface states at the top of the O(2p) band. Unoccupied states attributed to the band split off from the bottom of the conduction band also show considerable delocalization over the corner regions along the direction of the zig-zag, as well as over oxygen atoms which are behind the corner sites on the same terraces.

The electron densities associated with the F-center state at the step and the reverse corner are qualitatively rather similar to what we have already shown for the flat (001) surface. As in that case, the density is strongly localized at the F-center site, with substantial weights on neighboring oxygens. The height of the peak in the density at the reverse corner F-center site is almost identical to that found at the surface F-center, as might be expected since both sites have the same coordination. The height of the peak at the step F-center site is about 30 percent lower. On the other hand, the density associated with the corner F-center state shows considerable delocalization as demonstrated in Fig. 13.

6 Discussion

We first comment on the relaxed structure and the electronic structure of the MgO surface without F-centers. Our results for the flat (001) surface confirm what is already known from LEED [61, 62, 63] measurements, from previous *ab initio* [16] and semiempirical quantum calculations [65], and from modelling based on interaction models [7, 64] that relaxation effects are extremely small, and consist mainly of rumpling, with O ions moving slightly out of the surface and Mg ions moving slightly in. However, we have shown that relaxation effects are far larger at the step, corner and reverse corner, and are associated with large energy reductions. The ionic displacements are such as to smooth out the surface irregularity. This is easy to understand since the (001) surface of MgO crystal is the most stable one [1, 9, 65].

Our displacements agree qualitatively with the displacements obtained in the model-based calculations [7, 8, 9], but in the absence of published quantitative results from the latter work we are unable to make detailed comparisons.

The most important new information from this part of our work concerns the surface electronic states. We have shown that there is a substantial narrowing of the band-gap at the flat (001) surface by ca. 1.6 eV, and that this is entirely due to the formation of surface states at the bottom of the conduction band. We find no surface states above the top of the valence band, and nor do we find any surface states associated with the O(2s) band. These findings are in accord with recent LMTO LDA work [14] where detailed calculations of the band structure of the (001) MgO surface have been done. Surface states pulled down from the CBM have been found there, the bottom of this band lying ca. 0.6 eV below the bottom of the bulk conduction band. Our results on the predominant localization on surface oxygens of the surface states associated with the bottom of the conduction band support recent theoretical semiempirical calculations [72]. Namely, it was shown that surface excitonic transitions in MgO are of the one-center-type, i.e. are mainly localised on surface oxygen atoms.

According to our calculations, the DOS of the perfect step is essentially the same as for the flat surface, but important new features appear for the corner - reverse corner system. First, a prominent band of surface states splits off from the O(2s) band. The existence of this type of surface state is well known from *ab initio* calculations on other oxides such as TiO₂ [68]. In the present case, it seems to exist only at corners, and this suggests that it could be used as an experimental tool for detecting the presence of corners. The second new feature is the appearance of surface states above the bulk VBM, which leads to a further narrowing of the surface band-gap by ca. 0.8 eV below its value for the flat surface. This might also be used as an experimental tool for detecting corners.

The systematic reduction of surface band-gap as one passes from the bulk to the flat (001) surface and then to the corner irregularity may already have been observed in the UV diffuse reflectance spectroscopy [4], which indicates a series of peaks below the fundamental absorption edge (which was found to be at 8.7 eV). First two peaks at 4.62 eV and 5.75 eV have been attributed to bound (localised) excitonic transitions near 3-fold (corners) and 4-fold (steps) surface oxygens. Another two peaks at 6.6 eV and 7.7 eV have been associated with free excitons on the flat surface and in the bulk, respectively. These experimental observations are generally consistent with what we have obtained in our calculations on the flat surface and various surface irregularities. The same trend for the band gap was also found in DV-X _{α} cluster calculations [3].

Turning now to our results for the F-center, we note first that our calculated properties of the bulk F-center are in close agreement with the previous calculations of Wang and Holzwarth [28]. Our finding that the bulk F-center level lies 2.7 eV above the VBM is very similar to their energy of 2.3 eV, and our conclusions about the strong localization of the total electron density at the F-center site but the much weaker localization of the density associated with the F-center level are in complete agreement with what they find. We also agree about the almost total absence of relaxation effects.

The new information we have added is that the results are completely independent of the size of repeating cell, provided the number of sites is at least 16. We can therefore regard our results as referring to an isolated F-center in an infinite crystal.

Our calculated value of 10.5 eV for the bulk oxygen removal energy can be related to the F-center formation energy Q defined as the oxygen removal energy minus the cohesive energy per formula unit with respect to free atoms [28, 67]. Using our calculated cohesive energy of 11.1 eV, we obtain the value $Q = -0.6$ eV. The calculations of Wang and Holzwarth [28] gave the value $Q = -0.4$ eV. In principle, Q can be measured by additive coloring experiments in which the equilibrium between bulk F-centers and Mg vapour is studied as a function of temperature and pressure. There has been only one attempt [56] to measure Q for MgO, which gave the value 1.5 eV. The calculated values obtained both by us and by Wang and Holzwarth are clearly in poor agreement with this. However, substantial errors are quoted in the experimental measurements, and we believe that the measured Q is subject to an error of at least ± 0.8 eV. In addition, there may well have been systematic errors due to lack of equilibration between bulk and vapor. We therefore believe that this disagreement is not necessarily due to inaccuracy in the calculations.

Our calculations have shown the expected reduction of oxygen removal energy as the coordination number of the oxygen site decreases through the sequence: bulk, flat surface, reverse corner, step, corner. The removal energy actually decreases rather little, being only 2.5 eV or 20 % lower at the corner than it is in the bulk. Other properties of the F-center also seem to depend rather weakly on its location. As we go from the bulk to the flat surface, the degree of localization of the F-center electron density (as measured by the value of the density at the F-center site) scarcely changes, the energy of the F-center level decreases by only 0.4 eV, and relaxation effects continue to be negligible. The further changes in electron distribution and the energy of the F-center level on going to the step site are almost negligible. It is only on going to the corner and reverse corner sites that significant changes occur. Namely, the F-center level is found surprisingly close to the top of the valence band for the 5-fold coordinated reverse corner system (0.8 eV). However, as follows from our calculations, for the 3-fold coordinated corner system, for which the F-center electronic density is substantially delocalised, its level is further pulled up by 0.9 eV.

Acknowledgments

The work of LNK and JMH is funded by EPSRC grants GR/J37546 and GR/H67935. The work of LNK was also supported in part by the Latvian Scientific Council, grant 93.270. The calculations were performed using an allocation of time on the Cray T3D at EPCC provided by the High Performance Computing Initiative. For assistance in enhancing the speed of the CETEP code we are indebted to Dr. I. Bush of Daresbury Laboratory. Analysis of the results was performed using local distributed hardware funded by EPSRC grants GR/H31783 and GR/J36266. We gratefully acknowledge

useful discussions with Prof. R. Joyner, Prof. A. M. Stoneham FRS, Dr. A. H. Harker, Dr. A. L. Shluger, Prof. Dr. J.-M. Spaeth and Dr. R. Williams.

References

- [1] V. E. Henrich and P. A. Cox, *The Surface Science of Metal Oxides* (Cambridge Univ. Press, 1994).
- [2] V. E. Henrich, Rep. Prog. Phys. **48** (1985) 1481.
- [3] M. Tsukada, H. Adachi, and C. Satoko, Progr. in Surf. Sci. **14** (1983) 113.
- [4] E. Garrone, A. Zecchina, and F. S. Stone, Phil. Mag. B **42** (1980) 683.
- [5] S. Ferrer, J. M. Rojo, M. Salmeron, and G. A. Somorjai, Phil. Mag. A **45** (1982) 261.
- [6] S. Coluccia, A. Barton, and A. J. Tench, J. Chem. Soc. Faraday Trans. I **77** (1981) 2203.
- [7] W. C. Mackrodt, J. Chem. Soc. Faraday Trans. II **85** (1985) 541.
- [8] E. A. Colbourn, J. Kendrick, and W. C. Mackrodt, Surf. Sci. **126** (1983) 550.
- [9] P. W. Tasker and D. M. Duffy, Surf. Sci. **137**, 91 (1984).
- [10] V. Puchin, A. Shluger, Y. Nakai, and N. Itoh, Phys. Rev. B **49** (1994) 11364.
- [11] J. Goniakowski and C. Noguera, Surf. Sci. ,submitted.
- [12] A. L. Shluger, J. D. Gale, and C. R. A. Catlow, J. Phys. Chem. **96** (1992) 10389.
- [13] W. Langel and M. Parrinello, Phys. Rev. Lett. **73** (1994) 504.
- [14] U. Schönberger and F. Aryasetiawan, Phys. Rev. B, submitted.
- [15] S. Pugh and M. J. Gillan, Surf. Sci. **320** (1994) 331.
- [16] M. Causà, R. Dovesi, C. Pisani, and C. Roetti, Surf. Sci. **175** (1986) 551.
- [17] M. Causà, R. Dovesi, E. Kotomin, and C. Pisani, J. Phys. C: Solid State Phys. **20** (1987) 4983.
- [18] A. Gibson, R. Haydock, and J. P. LaFemina, J. Vac. Sci. Technol. A **10** (1992) 2361.
- [19] C. A. Scamehorn, N. M. Harrison, and M. I. McCarthy, J. Chem. Phys. **101** (1994) 1547.

- [20] G. P. Srivastava and D. Weaire, *Adv. Phys.* **36** (1987) 463.
- [21] M. J. Gillan, in *Proc. NATO ASI on Computer Simulation in Material Science, Aussois, March 1991*, ed. M. Meyer and V. Pontikis, p. 257 (Dordrecht, Kluwer, 1991)
- [22] M. C. Payne, M. P. Teter, D. C. Allan, T. A. Arias, and J. D. Joannopoulos, *Rev. Mod. Phys.* **64** (1992) 1045.
- [23] I. Manassidis and M. J. Gillan, *J. Am. Ceram. Soc.* **77** (1994) 335.
- [24] I. Manassidis, A. De Vita, and M. J. Gillan, *Surf. Sci.* **285** (1993) L517.
- [25] A. De Vita, I. Manassidis, J.-S. Lin, and M. J. Gillan, *Europhys. Lett.* **19** (1992) 605.
- [26] A. De Vita, M. J. Gillan, J. S. Lin, M. C. Payne, I. Štich, and L.J.Clarke, *Phys. Rev. B* **46** (1992) 12964.
- [27] K. J. Chang and M. L. Cohen, *Phys. Rev. B* **30** (1984) 4774.
- [28] Q. S. Wang and N. A. W. Holzwarth, *Phys. Rev. B* **41** (1990) 3211.
- [29] B. M. Klein, W. E. Pickett, L. L. Boyer, and R. Zeller, *Phys. Rev. B* **35** (1987) 5802.
- [30] K. Jackson, M. R. Pederson, and B. M. Klein, *Phys. Rev. B* **43** (1991) 2364.
- [31] A. Gibson, R. Haydock, and J. LaFemina, *Phys. Rev. B* **50** (1994) 2582.
- [32] Yong-Nian Xu and W. Y. Ching, *Phys. Rev. B* **43** (1991) 4461.
- [33] R. Car and M. Parrinello, *Phys. Rev. Lett.* **55** (1985) 2471.
- [34] L. J. Clarke, I. Štich, and M. C. Payne, *Comp. Phys. Commun.* **72** (1992) 14.
- [35] L. Kleinman and D. M. Bylander, *Phys. Rev. Lett.* **48** (1980) 566.
- [36] R. D. King-Smith, M. C. Payne, and J. S. Lin, *Phys. Rev. B* **44** (1991) 13063.
- [37] D. M. Ceperley and B. J. Alder, *Phys. Rev. Lett.* **45** (1980) 566.
- [38] J. Perdew and A. Zunger, *Phys. Rev. B* **23** (1981) 5048.
- [39] H. J. Monkhorst and J. D. Pack, *Phys. Rev. B* **13** (1976) 5188.
- [40] R. W. G. Wyckoff, *Crystal Structures*, 2nd ed., Vol. 2 (Interscience, New York, 1964) ch. 5.
- [41] G. Lehmann and M. Taut, *Phys. Stat. Sol.* **54** (1972) 469.

- [42] O. Jepsen and O. K. Andersen, Solid State Comm. **9** (1971) 1763.
- [43] P. E. Blöchl, O. Jepsen, and O. K. Andersen, Phys. Rev. B **49** (1994) 16223.
- [44] C. E. Moore, *Atomic Energy Levels*, Nat. Bur. Stand. (U.S.) Ref. Data Ser. No. 35 (U.S. GPO, Washington, D.C., 1971), Vol. I, p.45.
- [45] O. E. Taurian, M. Springborg, and N. E. Christensen, Solid State Comm. **55** (1985) 351.
- [46] *CRC Handbook of Chemistry and Physics*, 60th ed., edited by R. C. Weast and M. J. Astle (Chemical Rubber Co., Boca Raton, FL, 1980), p. D-72.
- [47] J. Vail, J. Phys. Chem. Solids **51** (1990) 589.
- [48] R. Pandey and J. Vail, J. Phys. C: Cond. Matter **1** (1989) 2801.
- [49] A. B. Sobolev, V. A. Lobach, and B. V. Shul'gin, Sov. Phys. Solid State **27** (1986) 1881.
- [50] R. Pandey, J. E. Jaffe, and A. B. Kunz, Phys. Rev. B **43** (1991) 9228.
- [51] S. P. Kowalczyk, F. R. McFeely, L. Ley, V. T. Gritsyna, and D. A. Shirley, Solid State Comm. **23** (1977) 161.
- [52] L. Fiermans, R. Hoogewijs, G. de Mayer, and J. Vennik, Phys. Status Solidi A **59** (1980) 569.
- [53] M. L. Bortz, R. G. French, D. J. Jones, R. V. Kasowski, and F. S. Ohuchi, Phys. Scr. **41** (1990) 537.
- [54] D. W. Fisher, Adv. X-ray Analysis **13** (1970) 159.
- [55] D. M. Roessler and W. C. Walker, Phys. Rev. **159** (1967) 733.
- [56] L. A. Kappers, R. L. Kroes, and E. B. Hensley, Phys. Rev. B **1** (1970) 4151.
- [57] Y. Chen, V. M. Orera, R. Gonzalez, R. T. Williams, G. P. Williams, G. H. Rozenblatt, and G. J. Pogatshnik, Phys. Rev. B **42** (1990) 1410.
- [58] Y. Chen, J. L. Kolopys, and W. A. Sibley, Phys. Rev. **186** (1969) 865.
- [59] G. P. Summers, T. M. Wilson, B. T. Jeffries, H. T. Tohver, Y. Chen, and M. M. Abraham, Phys. Rev. B **27** (1983) 1283.
- [60] G. H. Rosenblatt, M. W. Rowe, G. P. Williams, Jr., and R. T. Williams, Phys. Rev. B **39** (1989) 10309.
- [61] T. Urano, T. Kanaji, and M. Kaburagi, Surf. Sci. **134** (1983) 109.

- [62] D. L. Blanchard, D. L. Lessor, J. P. LaFemina, D. R. Baer, W. K. Ford, and T. Guo, *J. Vac. Sci. Technol. A* **9** (1991) 1814.
- [63] W. R. Welton-Cook and W. Berndt, *J. Phys. C: Solid State Phys.* **15** (1982) 5691.
- [64] A. J. Martin and H. Bilz, *Phys. Rev. B* **19** (1979) 6593.
- [65] J. Goniakowski and C. Noguera, *Surf. Sci.* **323** (1995) 129.
- [66] V. E. Henrich, G. Dresselhaus, and H. J. Zeiger, *Phys. Rev. B* **22** (1980) 4764.
- [67] A. Gibson, R. Haydock, and J. P. LaFemina, *Appl. Surf. Sci.* **72** (1993) 285.
- [68] D. Vogtenhuber, R. Podloucky, A. Neckel, S. G. Steinemann, and A. J. Freeman, *Phys. Rev. B* **49** (1994) 2099.
- [69] J. Magill, J. Bloem, and R. W. Ohse, *J. Chem. Phys.* **76** (1982) 6227.
- [70] V. T. Coon, *Surf. Sci.* **88** (1979) L42.
- [71] V. M. Bermudez, *Surf. Sci.* **74** (1978) 568.
- [72] A. L. Shluger, R. W. Grimes, C. R. A. Catlow, and N. Itoh, *J. Phys.: Condens. Matter* **3** (1991) 8027.

Table 1. Calculated oxygen removal energies (in eV) for both unrelaxed and relaxed F-center systems of various sizes of the repeating cells in the bulk of MgO crystal.

number of atoms in the cell	unrelaxed	relaxed
8	10.656	-
16	10.554	10.553
32	10.579	10.571
54	10.568	10.560
64	10.568	10.547

Table 2. Oxygen removal energies (in eV) for both unrelaxed and relaxed surface F-center in various positions with respect to the surface using calculations on 2-layer, 4-layer and 6-layer slabs.

number of layers in the slab	The F-center position					
	1st layer		2nd layer		3rd layer	
	unrelaxed	relaxed	unrelaxed	relaxed	unrelaxed	relaxed
2	9.618	9.556	-	-	-	-
4	9.801	9.759	10.396	10.397	-	-
6	9.811	9.768	10.416	10.414	10.524	10.514

Table 3. Displacements of ions shown in Fig. 8a at the perfect step and around the F-center at the step given in units of the nearest neighbors O - Mg distance in the perfect lattice $d = 2.082 \text{ \AA}$.

Ion	Type	Perfect step		F-center system		
		x	z	x	y	z
1	Mg	0.12	0.02	0.11	-0.07	0.06
2	O	0.09	0.05	-	-	-
3	Mg	0.04	-0.01	0.07	0.0	0.01
4	O	0.05	0.0	0.05	0.01	0.0
5	O	-0.03	0.06	-0.02	0.01	0.07
6	Mg	-0.04	0.07	-0.03	0.0	0.06

Table 4. Displacements of ions shown in Fig. 8b at the perfect corner - reverse corner system as well as for the same systems with F-center at the corner and the reverse corner positions, given in units of the nearest neighbors O - Mg distance in the perfect lattice $d = 2.082 \text{ \AA}$.

Ion	Type	Perfect system			F-center at					
					the corner			the reverse corner		
		x	y	z	x	y	z	x	y	z
1	O	-0.04	-0.04	0.03	0.02	0.02	0.01	-	-	-
2	Mg	0.01	0.11	0.00	0.07	0.07	0.05	0.0	0.08	0.04
3	O	0.11	0.11	0.06	-	-	-	0.10	0.10	0.05
4	Mg	-0.01	-0.01	0.00	0.0	0.0	0.01	-0.01	-0.01	-0.04
5	O	0.00	-0.02	0.02	-0.01	-0.01	0.04	0.02	-0.01	0.02
6	Mg	-0.04	-0.04	0.13	-0.02	-0.02	0.01	-0.02	-0.02	0.13
7	Mg	0.01	0.02	-0.02	0.02	0.02	-0.01	0.02	0.07	-0.01
8	O	0.06	0.06	0.00	0.03	0.03	0.01	0.06	0.06	0.01

Table 5. Oxygen removal energies (in eV) for unrelaxed and relaxed F-center at the step, the corner and the reverse corner systems.

type of irregularity	nn [†]	nnn [‡]	unrelaxed	relaxed
step	4	5	8.931	8.997
corner	3	3	7.012	8.058
reverse corner	5	7	9.205	9.367

[†] Number of nearest Mg ions around the vacancy

[‡] Number of nearest oxygen ions around the vacancy

Figure captions

Fig. 1. Electronic DOS of the perfect bulk crystal (top panel) and the 16-site (middle panel) and 54-site (bottom panel) bulk F-center systems. Arbitrary units are used for the DOS.

Fig. 2. A contour plot of the valence electronic density of the 54-site F-center system (in units of 10^{-2} electron/ \AA^3). The cut has been made in the (001) plane. To avoid high peaks on oxygens, the density has been chopped at 0.2 electron/ \AA^3 . The positions of oxygen atoms are indicated by the symbol X. Distances are in \AA .

Fig. 3. The dependence of $\Delta n(R)$ (see Eq.(2)) for the 54-site F-center system on the sphere radius R (see text for details).

Fig. 4. A contour plot of the electronic density associated with the F-center band for the 54-site F-center system. Positions of Mg atoms are indicated by the symbol Δ . The units and other notations are the same as in Fig. 2.

Fig. 5. The total DOS of the unrelaxed six-layer slab (top panel) and the flat surface systems containing third layer (middle panel) and first layer (bottom panel) F-centers. Arbitrary units are used for the DOS.

Fig. 6. A contour plot of the fictitious charge density (see Eq. (3)) associated with the first unoccupied state at the bottom of the conduction band of the flat surface. The cut has been made parallel to the surface normal through nearest surface Mg and O ions. The top two layers of atoms are shown explicitly. The units and notations are as in Fig. 4.

Fig. 7. The contour plot of the valence electronic density of the flat surface system containing the first-layer F-center. The cut has been made along the direction of the surface normal through the F-center and nearest Mg ions on the surface. Other notations and units are the same as in Fig. 2.

Fig. 8. Repeating geometries used in the *ab initio* calculations for the step (a) and the corner - reverse corner (b) systems. Mg and O atoms are indicated by grey and white circles, respectively. In each case, only upper side of the slab is shown. Note that the axes of the Cartesian coordinate system are also shown for each case. They correspond to Eqs.(4) and (5). Corresponding F-center systems have been created by removing oxygen atoms 2 (a), 3 or 1 (b) in the case of the step, corner and reverse corner systems, respectively.

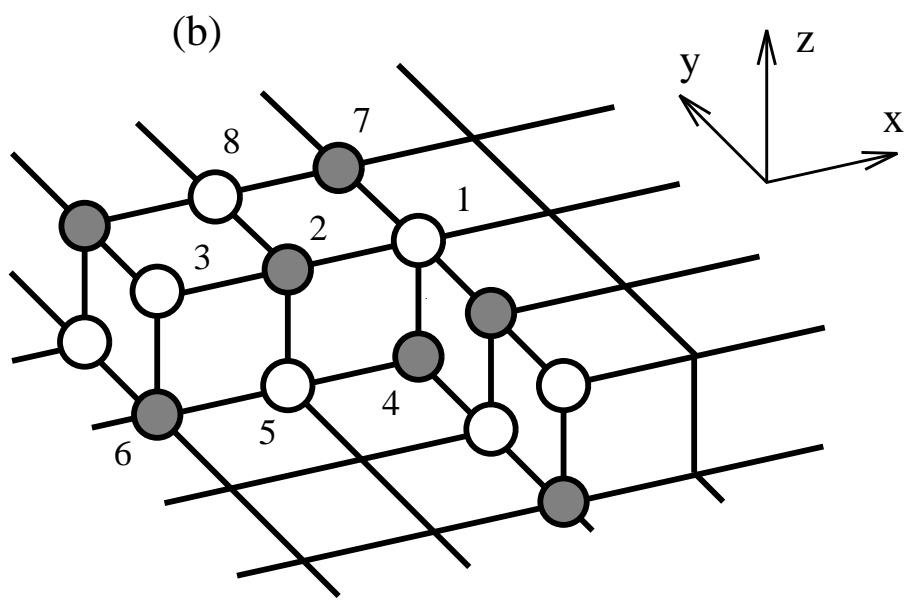
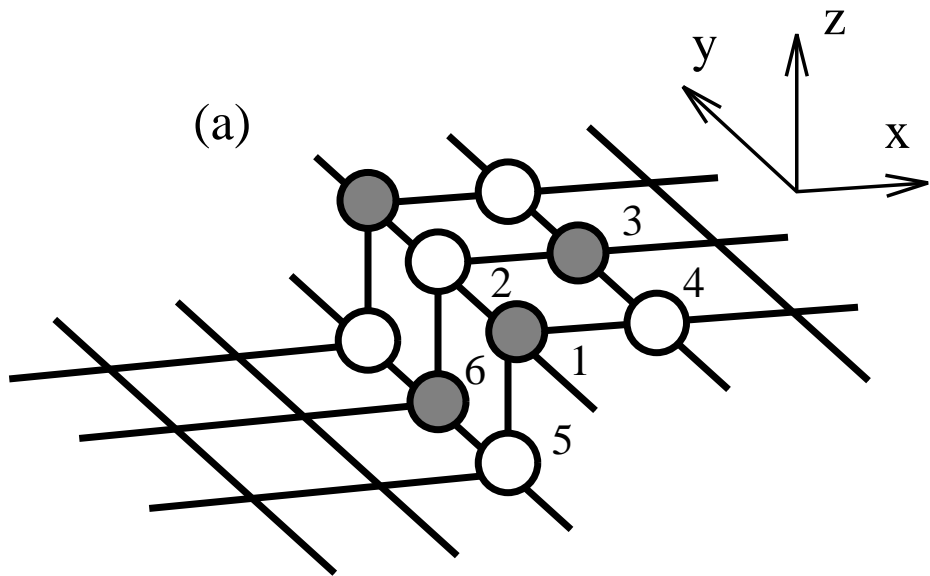
Fig. 9. The electronic DOS of the perfect corner - reverse corner system (top panel), the system containing the F-center at the corner (middle panel) and the reverse corner (bottom panel). Arbitrary units are used for the DOS.

Fig. 10. A contour plot of the fictitious charge density (see Eq. (3)) associated with the band of unoccupied states split off from the the bottom of the conduction band of the perfect corner - reverse corner system. The cut has been made in a plane parallel to the terraces passing through the corners along the zig-zag step. Other notations and units are the same as in Fig. 4.

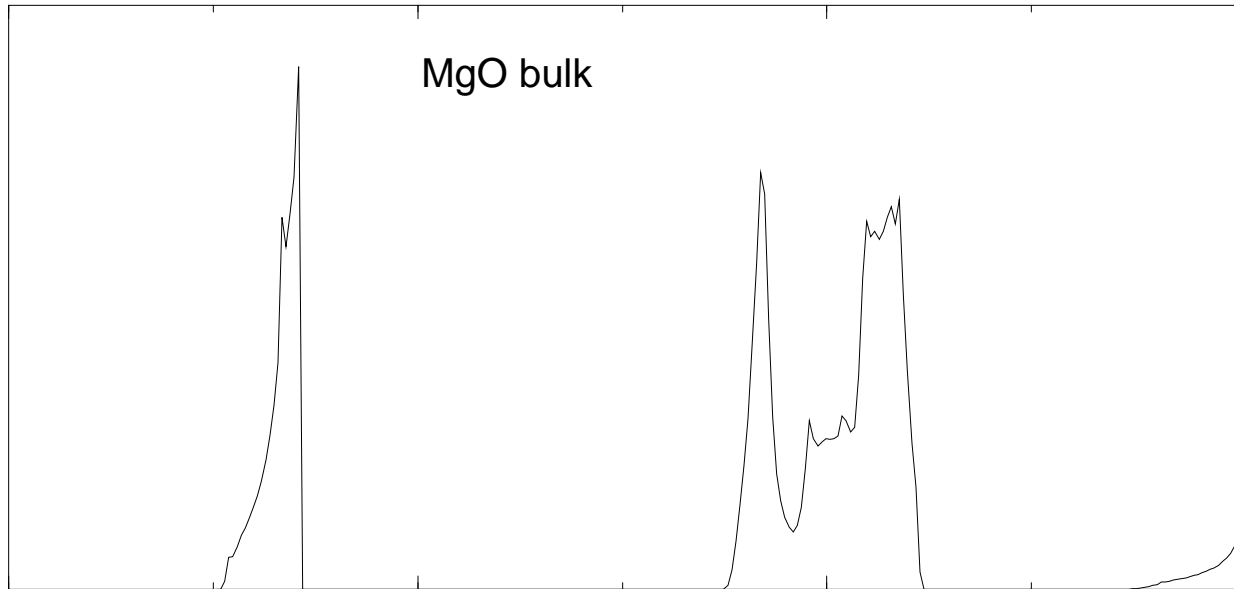
Fig. 11. A contour plot of the total valence electronic density for the perfect corner - reverse corner system. The cut is the same as in Fig. 10. Other notations and units are the same as in Fig. 2.

Fig. 12. The electronic DOS for the system containing the F-center at the step. Arbitrary units are used for the DOS.

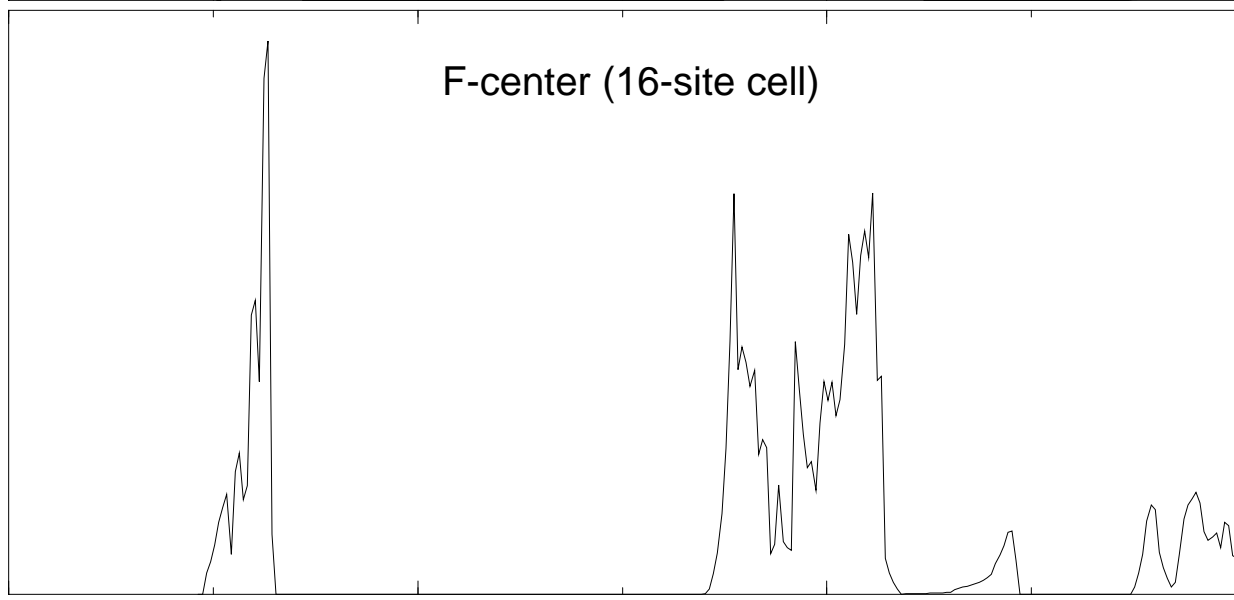
Fig. 13. A contour plot of the electronic density associated with the F-center band for the corner F-center system. The cut is the same as in Fig. 10. Other notations and units are the same as in Fig. 4.



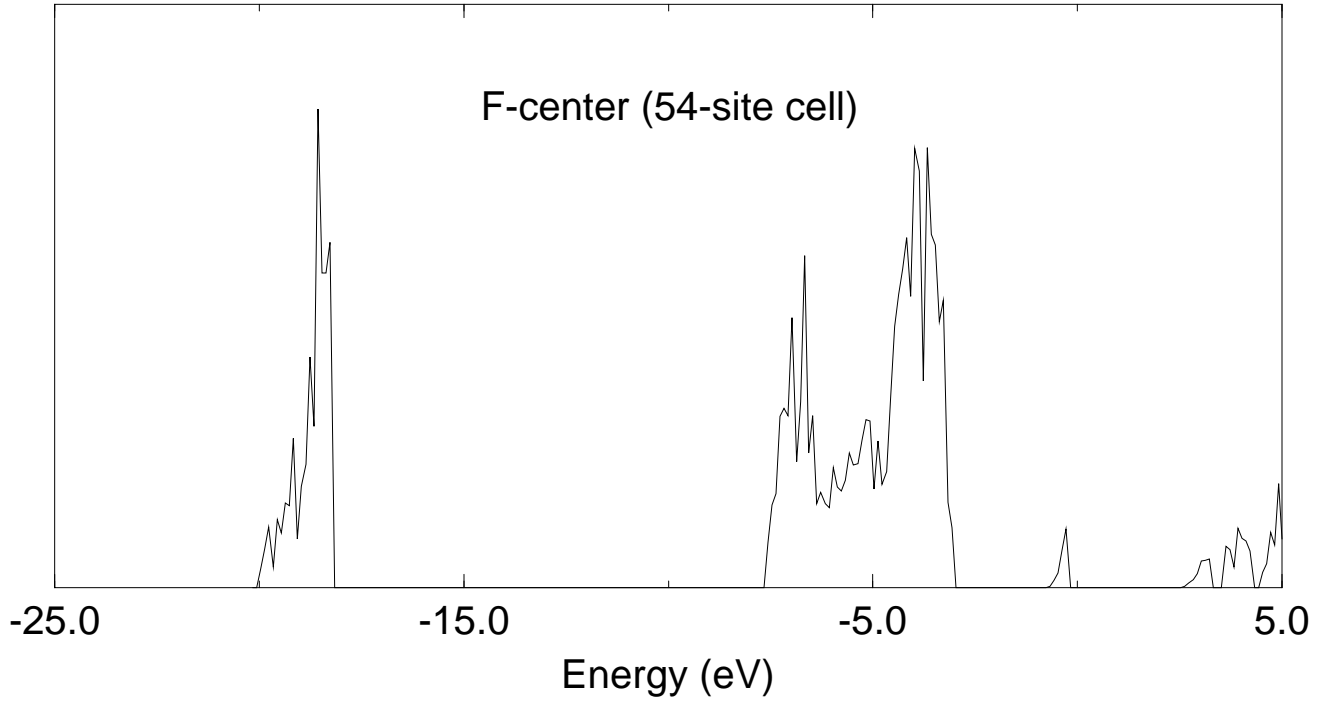
MgO bulk

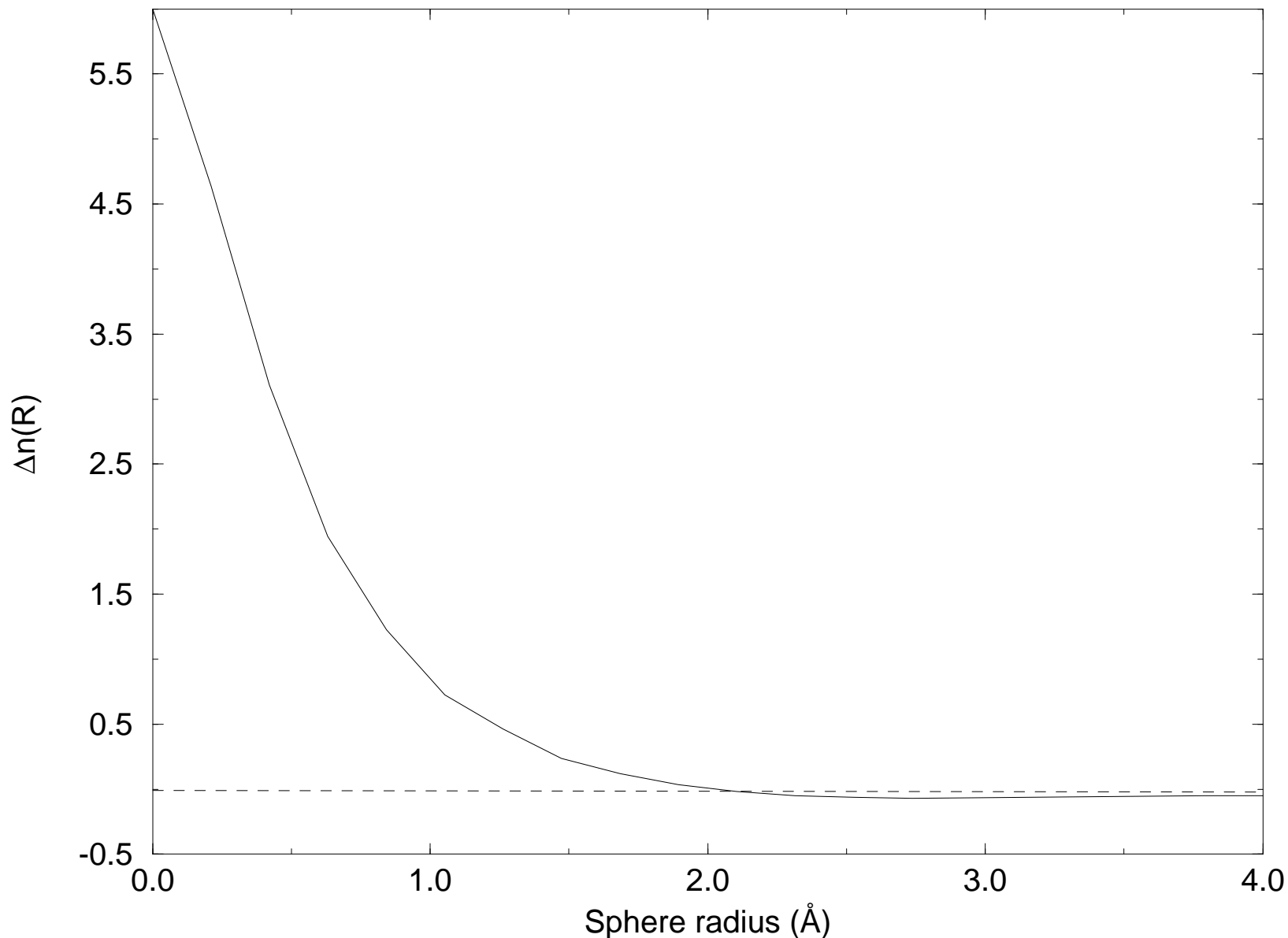


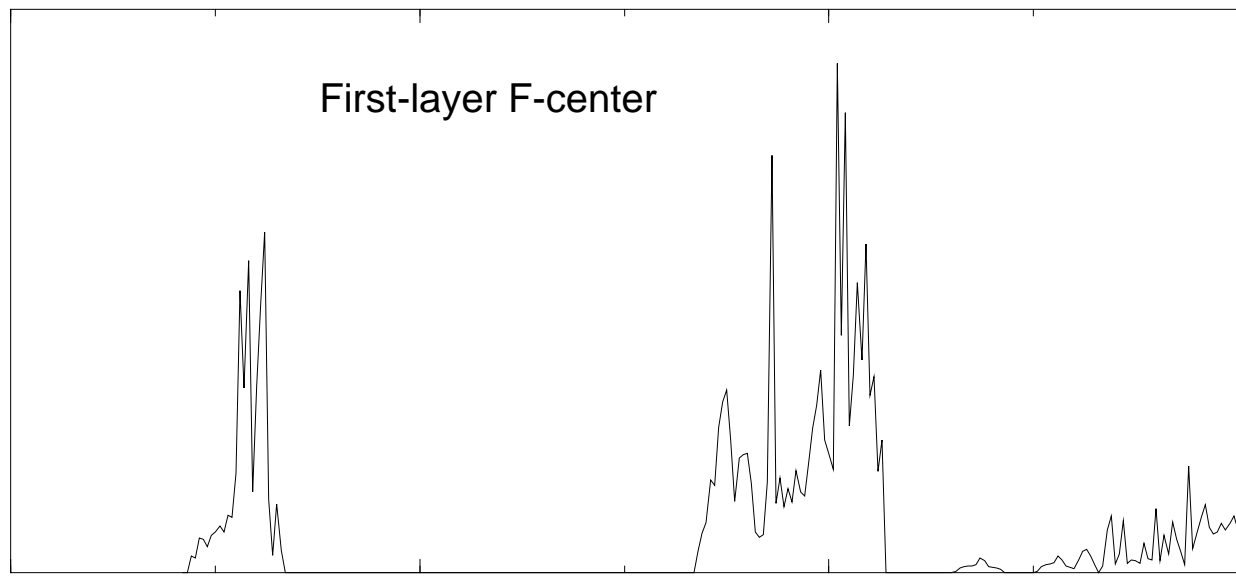
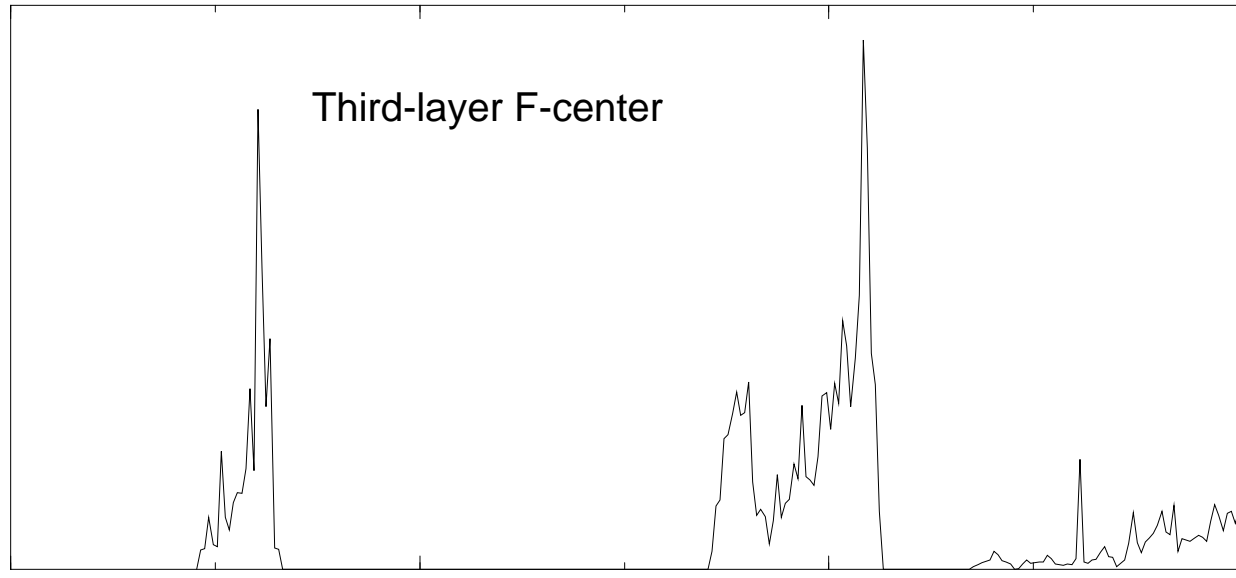
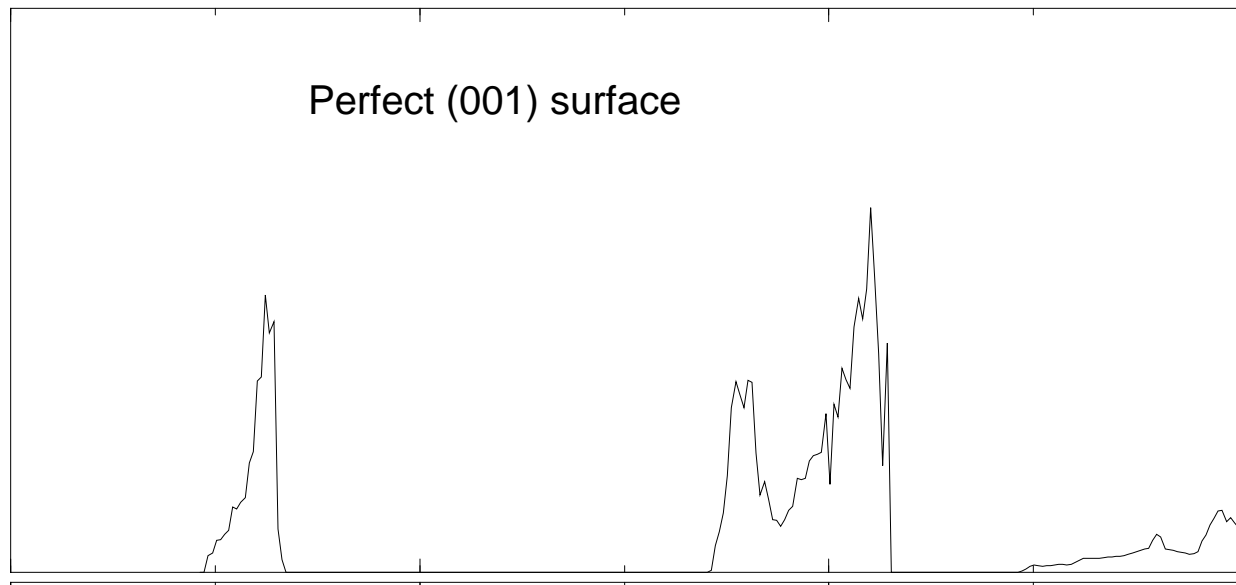
F-center (16-site cell)



F-center (54-site cell)

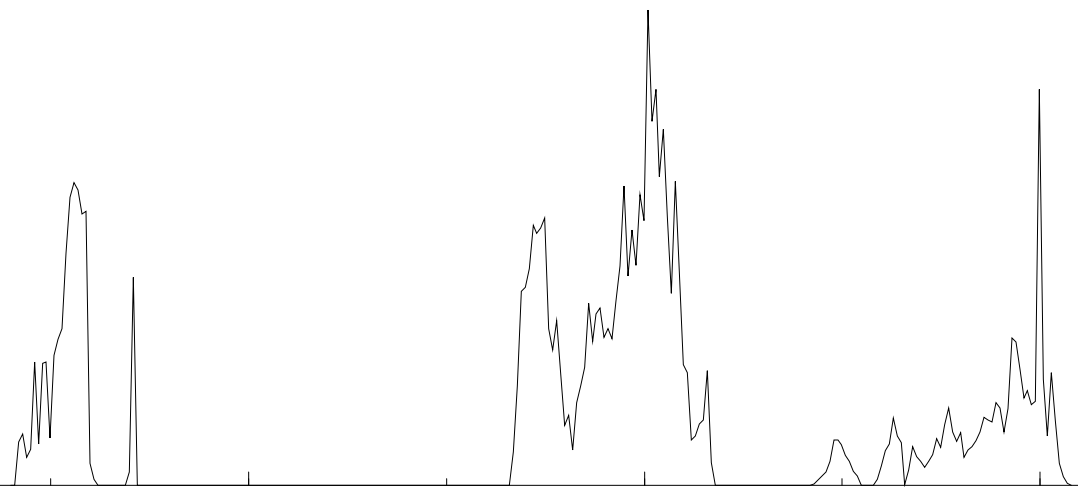




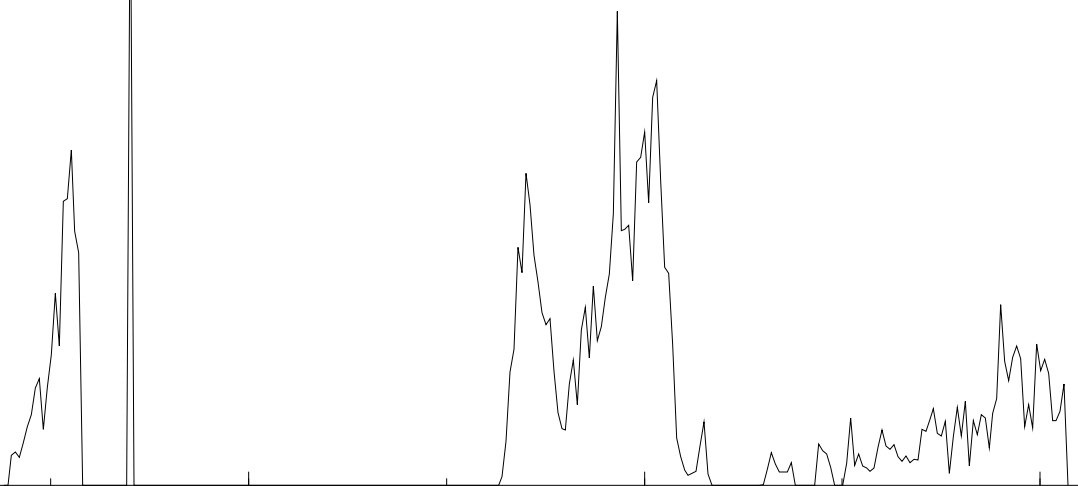


-25.0 -15.0 -5.0 5.0
Energy (eV)

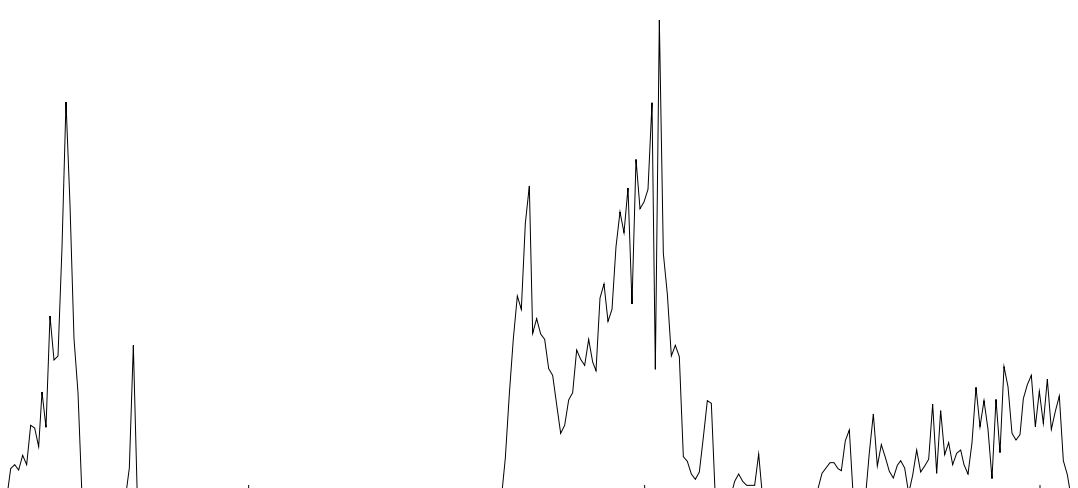
Perfect corner - reverse corner system



F-center at the corner



F-center at the reverse corner



-25.0

-15.0

-5.0

5.0

Energy (eV)

F-center at the step

